IEEE Access
Multidisciplinary | Rapid Review | Open Access Journal

SPECIAL SECTION ON ARTIFICIAL INTELLIGENCE FOR PHYSICAL-LAYER WIRELESS COMMUNICATIONS

Received October 7, 2019, accepted October 25, 2019, date of publication October 29, 2019, date of current version November 11, 2019.

Digital Object Identifier 10.1109/ACCESS.2019.2950127

Deep-Learning-Aided Cross-Layer Resource Allocation of OFDMA/NOMA Video Communication Systems

SHU-MING TSENG[1], YUNG-FANG CHEN[2], CHENG-SHUN TSAI[1], AND WEN-DA TSAI[3]

[1]Department of Electronic Engineering, National Taipei University of Technology, Taipei 106, Taiwan
[2]Department of Communication Engineering, National Central University, Taoyuan 320, Taiwan
[3]Compal Electronics, Inc., Taipei 114, Taiwan

Corresponding author: Shu-Ming Tseng (shuming@ntut.edu.tw)

This work was supported by the Ministry of Science and Technology, Taiwan, under Grant MOST 108-2221-E-027-033.

ABSTRACT In previous study, deep learning and autoencoder have been applied for data detection of NOMA systems, rather than the resource allocation of OFDMA/NOMA systems. In previous work, we proposed the use of non-deep-learning-based cross-layer resource allocation for OFDMA/NOMA video communication systems. In this paper, we apply a deep neural network and supervised learning to an OFDMA subcarrier assignment and NOMA user grouping problem in downlink video communication systems. The resource allocation results from our previous work are used as training data at the training stage. At the testing stage, we propose a conversion algorithm to map the result of the sigmoid activation function (values between [0,1]) of the output layer of the DNN to either zero (unassigned) or one (assigned), in order to meet two hard constraints. The PSNR performance is very close (within 0.2dB) to that but has lower complexity, due to the non-iterative approach used in the testing stage of the DNN.

INDEX TERMS Deep neural network, supervised learning, multi-label classification, application layer, physical layer, OFDMA, NOMA, multimedia communications.

I. INTRODUCTION

In recent years, non-orthogonal multiple access (NOMA) has emerged [1], [2] and is now used in the 3GPP standard [3] and the digital television standard ATSC 3.0 [4]. NOMA adds an additional power dimension and thus allows multiple users to occupy one orthogonal multiple access (OMA) resource block. The bandwidth efficiency is thus increased [5]. NOMA is one of the key enabling technologies for 5G ultra-reliable low-latency communications [6], [7] since it decreases latency by supporting many more users than OMA [8]. Since IP video traffic is expected to account for 82% of all IP traffic (both business and consumer) by 2022, up from 75% in 2017 according to a recent Cisco report [9], it is important to improve the performance of NOMA multimedia transmissions.

NOMA systems can be divided into uplink (UL) and downlink (DL) systems. DL NOMA systems include [10], [11]. In [10], the performance and complexity tradeoff are considered in the resource allocation for DL NOMA systems. The NP hardness is proven, and Lagrangian duality and dynamic programming are proposed. The authors of [11] propose a resource allocation algorithm combining CoMP and NOMA to improve the data rate of edge cells. UL NOMA systems include [12], [13]. In [12], a greedy-based resource allocation was proposed for UL NOMA systems in order to maximize the total capacity. In [13], an optimal power allocation algorithm and a less complex sub-optimal clustering method are proposed to maximize the throughput. However, the above references only focus on the physical layer (Layer 1), and consider the allocation of resources from a single point of view.

Additionally, orthogonal frequency division multiple access (OFDMA) is used in Wi-Fi, 4G and 5G New Radio Phase I [6] due to its increased bandwidth efficiency, inter-symbol interference tolerance, and flexible resource allocation. In [14]–[16], the resources are allocated according to the channel state information (CSI) in the physical layer. On the other hand, [17]–[21] allocate the resources according to the rate distortion (RD) function

The associate editor coordinating the review of this manuscript and approving it for publication was Guan Gui.

in the application layer. Different users have different RD functions, and thus the total average video quality can be improved. In order to go beyond both the physical and application layers, the work in [22] proposes a cross physical/application layer resource assignment that jointly considers the application layer RD function and the physical layer CSI to minimize the total video distortion (mean square error, MSE) for UL OFDMA video transmission systems. Its average peak signal-to-noise ratio (PSNR, the video quality) outperforms prior schemes considering either the physical or application layers. References [23]–[25] extend [22] to Hybrid Automatic Repeat reQuest (HARQ), anti-jamming and multi-user multiple-input multiple-output (MU-MIMO) schemes, and maximize PSNR directly. However, [22]–[25] do not consider NOMA.

In our recent work [2], we propose the cross-layer resource allocation of DL OFDMA/NOMA video transmission systems to increase the average PSNR. Compared to [22], our proposed scheme adds NOMA, with two users rather than one on each subcarrier. Reference [2] first selects users according to [13], and the subcarriers are then iteratively reassigned to minimize the total video MSE of the application layer. Conversely, the suboptimal user grouping in [13] considers only the physical layer.

Deep learning is also widely used in many other areas, including speech recognition [26] (the first major industrial application), image classification [27], signal processing, communications and networks [28]. The concept of deep learning, a special type of algorithm in machine learning (ML), was proposed in 2006 [29]. Deep learning can be seen as feature learning from the perspective of artificial intelligence (AI) and a function approximation from a math or non-AI perspective. Deep learning is a part of machine learning and can handle big data and solve complex nonlinear optimization problems. It can be divided into three main categories: reinforcement learning, supervised learning, and unsupervised learning [30]. Reinforcement learning does not need a correct input-output pair (i.e. a right answer) but use a reward function to quantify its performance. Supervised learning exploits the labeled data and can overcome the above problems, while unsupervised learning tasks find patterns where the right answers are not known. A common example in communications is an auto-encoder, in which the unsupervised learning input to the network is the same as the output from the network. Deep learning uses a deep neural network (DNN) architecture, a computational model composed of more than one hidden layer, to learn to represent data with multiple abstraction levels, in a similar way to human brains. Deep learning can discover complicated structures in large training datasets by using the backpropagation algorithm to modify the internal neuron weights, which compute the representation in each layer from that in the previous layer [28].

The other deep learning architectures, the convolutional neural network (CNN) and the recurrent neural network (RNN), are special cases of DNN. CNN [31], [32] was developed to realize spatial correlations, and has shone light on the processing of images, video, speech and audio. Reference [27] represents a breakthrough by using CNN to halve the image classification error rate. RNN [33] was developed to realize temporal correlations, and has allowed for advances in sequential data such as machine translation [34]. Long short-term memory (LSTM), introduced in [35], is a special case of RNN that was designed to remember information for a longer period than RNN and to solve the vanishing gradient problem of RNN [30]. In the proposed resource allocation of OFDMA/NOMA video transmission systems, there are neither the spatial correlation addressed by CNN nor the temporal correlations assumed by RNN, and thus the fully connected DNN model is the most appropriate. The role of DNN is a tool to solve the classification task in resource allocation. For example, the resource allocation of an OFDMA system is to assign each OFDMA subcarrier (resource) to a user, and this is a classification task (either assigned or unassigned for each subcarrier/user pair).

II. RELATED WORK

Applications of deep learning in error correction codes and signal processing include the decoding of polar codes [36], an auto-encoder in the physical layer [37], an auto-encoder for the coding and decoding of sparse code multiple access (SCMA) [38], channel estimation and signal detection in OFDM [39], and an auto-encoder for data detection in NOMA [1]. After training, the computation time of the deep learning-based approach is between five and 11 times lower than that of non-deep learning approaches [38]. For radio resource allocation (time, subcarrier, power resource etc.), the focus of this paper is on a comparison of the existing works in this area using deep learning, as summarized in detail in Table 1 [40]–[42]. Note that unsupervised learning, such as an auto-encoder in the physical layer [37], SCMA [38], and data detection in NOMA [1], where the input to the network is same as the output from the network, is not applicable to radio resource allocation.

Previous studies of radio resource allocation (subcarrier/time slot assignment) have all addressed single-label classification problems, in which one subcarrier (channel) can be assigned (labeled) to only one user. With NOMA, however, one subcarrier (channel) can be assigned (labeled) to two users. Standard DNNs are not suitable for multi-label classification. One way to get around this is to consider all combinations of classes as separate classes. This causes combinatorial growth in the number of classes. In a limited training dataset, training many parameters causes over-fitting and thus poor results [43]. New methodologies must therefore be proposed for specific applications. Related papers include studies of smart meters [43], multi-speaker direction of arrival estimation [44], and offloading for mobile edge computing [45]. However, they do not use deep-learning-based multi-label classification for radio resource allocation in NOMA systems.

In this work, we apply deep-learning-based multi-label classification to OFDMA/NOMA systems to tackle the user

TABLE 1. Existing works on radio resource allocation using deep learning.

Publication	Learning method	Model	Goal and performance	Resources/NN output	NN input
[46]	Supervised	DNN	Maximize throughput in the Gaussian interference channel. The labeled data come from minimum mean square error (WMMSE).	Power	Channel coefficients
[47]	Reinforcement	Q-learning	Minimize the total power consumption of the i-th user's QoS constraints in cloud radio access networks. Decrease power consumption by 0-20% compared to single BS association and fully coordinated association	Power	Demand from users
[48]	Reinforcement	LSTM, special case of RNN	Maximize airtime allocated for LTE-U. Increase average airtime by about 18% compared to reactive approach.	Channel, time	Unlicensed channel
[49]	Reinforcement	Q-learning	Cooperative adaptive power allocation in D2D communications.	Power	Channel of all user pairs
[50]	Reinforcement	two fully connected DNN	Maximize spectrum efficiency (SE) in underlay cognitive radio network. Higher SE for a secondary user while interference to primary user is below a threshold.	Channel, power	Channel normalized to N(0,1)
[51]	Supervised	CNN	Maximize throughput via power control.	Power	Normalized channel
[52]	Reinforcement	Q-learning	Spectrum sharing with power control for secondary user.	Power	SINR
[53]	Supervised	DNN	Maximize energy efficiency through power control	Power	Channel
[54]	Supervised	DNN with unsupervised pre-training restricted Boltzmann machine (RBM)	Minimize the total transmitting power of the system while satisfying the QoS requirements of each user in terms of data rate and harvested power.	Time-switching ratios	Channel coefficient
[55]	Supervised	DNN	Optimize decoding order and power allocation of satellite NOMA downlink system.	Queue state channel state	Optimal decoding order
[56]	Reinforcement	Q-learning	Policy for channel switching with known system dynamics.	Previous action (channel)	Channel (may switch)
[57]	Reinforcement	Special NN	Minimize total SU interference subject to power and data rate constraints for OFDMA systems without NOMA.	Resource allocation requirement	Channel

grouping/subcarrier assignment in a cross-physical/ application layer fashion. We meet two of the 10 challenges of future research trends in deep learning for intelligent wireless networks: deep learning -based cross-layer design and deep learning -based application layer enhancement (QoS parameter PSNR) [40].

In this paper, we propose the cross-layer resource allocation of the DL OFDMA/NOMA video transmission system using DNN-based user grouping/subcarrier assignment. Our contributions are as follows:

1. We extend our previous work [2], an iterative cross-layer user grouping/subcarrier assignment/power allocation of the DL OFDMA/NOMA video transmission system, to the proposed DNN-based scheme by using deep learning-based cross-layer user grouping/subcarrier assignment (training set taken from [2]) and the same power allocation as in [2]. Following the training stage of DNN, the user grouping/subcarrier assignment is a direct mapping without iterations. This could decrease the complexity of resource allocation.

2. We replace only the building block with the most complexity, the cross-layer user grouping/subcarrier assignment, with a DNN-based one. To learn end-to-end communication systems, e.g. the auto-encoder in [1], [37], [38], the training

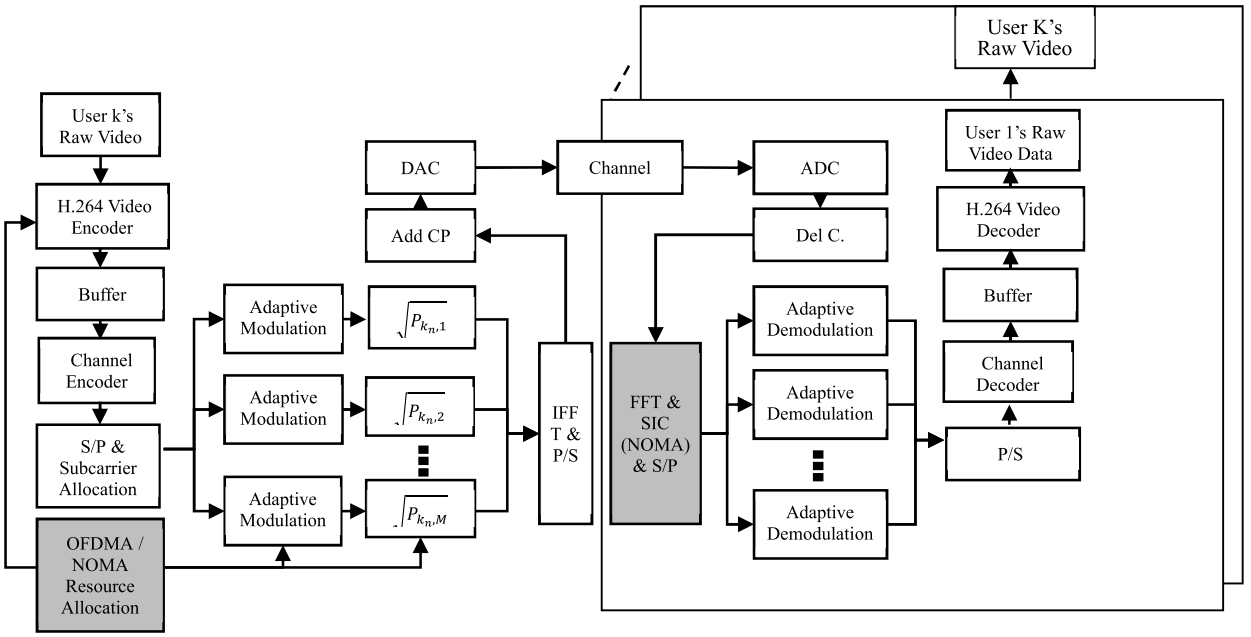

FIGURE 1. DL OFDMA/NOMA video transmission system.

complexity is prohibitive for long messages, because the auto-encoder needs to see each message (a total of 2^100 if the message length is 100) at least once [37]. This problem is serious for video communication, since the number of bits for one user in one GOP is often 10,000 or higher [22]–[24]. Augmenting only specific sub-task, cross-layer user grouping/subcarrier assignments in this paper is therefore more practical [37].

3. We formalize the OFDMA subcarrier assignment and NOMA user grouping tasks as a multi-label classification problem. This has been dealt with in other areas, such as smart meters, multi-speaker DOA, offloading for mobile edge computing, and image recognition [43–45], [58]. At the testing stage, we propose a conversion algorithm at the output layer to guarantee that the two hard constraints on the proposed DNN-based resource allocation algorithm are satisfied.

III. SYSTEM MODEL

A. OFDMA/NOMA SYSTEM BLOCK DIAGRAM

The OFDMA/NOMA video transmission system is shown in Fig. 1. The video transmission system is similar to that in [22], except for two gray boxes. The first of these is the OFDMA/NOMA resource allocation block, including NOMA user pairing, OFDMA subcarrier assignment, and power allocation among users sharing the same subcarrier, while the second is the successive interference cancellation (SIC). In the OFDMA/NOMA video transmission system, we have K users and M orthogonal subcarriers. The user index is k = {1,2,3…K}, and the subcarrier index is m = {1,2,3…M}.

B. NOMA SYSTEM MODEL FOR EACH SUBCARRIER

Fig. 2 shows the NOMA downlink system model for subcarrier m. We assume two users on one subcarrier.

The received signal is given by:

$$y_{m,k}^{DL} = H_{m,k}^{DL} \sum_{i=1}^{2} x_{m,i}^{DL} + n_{\mathrm{m,k}}^{DL}, \quad k = 1, 2, \tag{1}$$

where $n_{\mathrm{m,k}}^{DL}$ denotes the additive white complex Gaussian noise (AWGN) for subcarrier m, user k. $H_{m,1}^{DL}$ and $H_{m,2}^{DL}$ are the channel vectors for strong and weak users, respectively. $x_{m,1}^{DL} = \sqrt{\alpha_{m,1}^{DL}} s_{m,1}^{DL}$ and $x_{m,2}^{DL} = \sqrt{\alpha_{m,2}^{DL}} s_{m,2}^{DL}$ are the transmitted signals for strong users and weak users, respectively; $s_{m,1}^{DL}$ and $s_{m,2}^{DL}$ are the strong and weak user's signals, respectively; $\alpha_{m,1}^{DL}$ and $\alpha_{m,2}^{DL}$ are the power assignment factors, and $\alpha_{m,1}^{DL} + \alpha_{m,2}^{DL} = 1$. According to Equation (1), the signal received from the strong user on the m-th carrier is given by:

$$y_{m,1}^{DL} = H_{m,1}^{DL} x_{m,1}^{DL} + H_{m,2}^{DL} x_{m,2}^{DL} + n_{\mathrm{m,1}}^{DL}. \tag{2}$$

The strong user uses SIC to cancel out $H_{m,2}^{DL} x_{m,2}^{DL}$, the interference from the weak user. The strong user's signals can therefore be written as:

$$y_{m,1}^{DL} = H_{m,1}^{DL} x_{m,1}^{DL} + n_{\mathrm{m,1}}^{DL}. \tag{3}$$

Conversely, the weak user's received signal can be expressed as:

$$y_{m,2}^{DL} = H_{m,2}^{DL} x_{m,2}^{DL} + H_{m,2}^{DL} x_{m,1}^{DL} + n_{\mathrm{m,2}}^{DL}. \tag{4}$$

C. VIDEO MSE DISTORTION MODEL UNDER NOMA

For simplicity and accuracy, we use an empirical video distortion model like that in [22], [59], in the OMA systems. The difference is that ours has an interference term due to NOMA, specifically $P_{max} \alpha_{m,1}^{DL} \left| H_{m,1}^{DL} \right|^2$ in (6), which affects the $R_{k,m}^{DL}$ term in the video distortion expression (7).

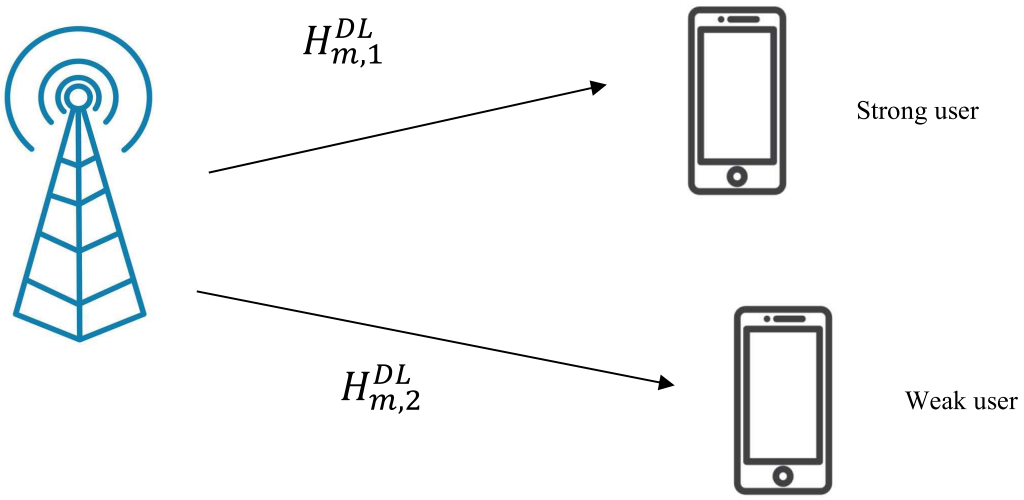

FIGURE 2. DL NOMA system model for subcarrier *m*.

We obtain a strong user information rate on the m-th subcarrier:

$$R_{m,1}^{DL}\left(\alpha_{m,1}^{DL}\right) = \mathrm{BW}*\log_2\left[1+\frac{\eta P_{max}\alpha_{m,1}^{DL}\left|H_{m,1}^{DL}\right|^2}{P_{N_0}^{DL}}\right], \quad (5)$$

where BW is the bandwidth of each subcarrier, $\eta = 3\left[Q^{-1}\left(\frac{SER_t}{4}\right)\right]^{-2}$, SER_t denotes the target symbol error rate, and we bring SER_t into the Q-function. $P_{N_0}^{DL}$ denotes the noise power, and P_{max} denotes the maximum power allowed per subcarrier. The weak user information rate on the m-th subcarrier is given by:

$$R_{m,2}^{DL}\left(\alpha_{m,2}^{DL}\right) = \mathrm{BW}*\log_2\left[1+\frac{\eta P_{max}\left(\alpha_{m,2}^{DL}\right)\left|H_{m,2}^{DL}\right|^2}{P_{max}\alpha_{m,1}^{DL}\left|H_{m,1}^{DL}\right|^2+P_{N_0}^{DL}}\right]. \quad (6)$$

Unlike in [22], the weak user information rate experiences interference from the strong user. Let MSE_k^{DL} be the rate distortion function for user k and $\sum_{m=1}^{M} R_{m,\mathrm{k}}^{DL}$ be the encoder rates in bits/s. Thus, for each group of pictures (GOP), the mean square error (MSE) video distortion can be modeled as [59]:

$$MSE_k^{DL} = a_k^{DL} + \frac{b_k^{DL}}{\sum_{m=1}^{M} R_{m,\mathrm{k}}^{DL} + c_k^{DL}}, \quad (7)$$

where a_k^{DL}, b_k^{DL} and c_k^{DL} are constants depending on the video. The video encoder rates are discrete values. These parameters are obtained by fitting the RD function by non-linear regression using operational points [22], [59].

D. AVERAGE PSNR

In the downlink the OFDMA/NOMA video transmission system, we need to maximize the average PSNR. The user k' PSNR is defined as $10\log_{10}\frac{255*255}{MSE_k}$ [22] and the average PSNR is the average of all users' PSNR. The video signal processing community has long been using mean squared error (MSE) and PSNR as fidelity metric (PSNR is defined a logarithmic representation of MSE, as described above). PSNR is a very good measure to evaluate and compare the video quality differences and are widely used because it is easy to calculate, has clear physical meanings, and is tractable for optimization purposes. The average SNR is no suited for the primary metric of video communications because the video distortion is video content dependent and different from a user to another but the noise is irrelevant of the video content of the different users.

E. OPTIMIZATION OF TOTAL VIDEO DISTORTION: PROBLEM FORMULATION

We want to maximize the total MSE, that is:

$$\min_{\underline{\underline{P}}} \sum_{k=1}^{K} \mathrm{MSE}_k^{DL}, \quad (8)$$

where $\underline{\underline{P}}$ is the K-by-M power allocation matrix whose element $P_{k,m}$ is the power assigned for user k on subcarrier m. The BS has a total power constraint P for all downlink users (conversely, each uplink user has a separate power constraint P). Each user must have at least one subcarrier, and each subcarrier is shared by two NOMA users. Thus, the optimization in (8) has the following constraints:

Constraint 1: Each user has at least one subcarrier.

Constraint 2: For $m \in \{1, 2, \ldots, M\}$, $S_m = \{k' | P_{k',m} \neq 0\}$, $||S_m|| = 2$, where $||S_m||$ denotes the set size of of S_m. That is, two users are assigned to subcarrier m.

Constraint 3: $\sum_{k=1}^{K} \sum_{m=1}^{M} P_{k,m} = \mathrm{P}$ for all k

Constraint 2 is nonconvex, meaning that the above optimization in (8) is NP hard. We proposed a suboptimal iterative algorithm in [2], as briefly described in Section IV.

IV. ITERATIVE CROSS-LAYER OFDMA/NOMA RESOURCE ALLOCATION ALGORITHM

Here, we briefly describe our previous work [2]. In this scheme, the subcarrier assignment/NOMA user grouping results are used as training data for deep-learning-based subcarrier assignment/NOMA user grouping in the next section. For details, readers are referred to [2].

1) Initial Subcarrier Allocation: First, the channel responses of all users on each subcarrier are sorted in descending order. The largest and smallest $\left|H_{m,k}^{DL}\right|^2$ values are found, and then this subcarrier m is assigned to these two users. In this step, only the physical layer channel state information (CSI) is considered.

2) Power Allocation And RD Function Slope Calculation: The power allocation on subcarrier m aims to decide the power assignment factors ($\alpha_{m,1}^{DL}$ and $\alpha_{m,2}^{DL}$) to minimize the sum of video distortion ($\mathrm{MSE}_{\mathrm{m},1}^{DL}+\mathrm{MSE}_{\mathrm{m},2}^{DL}$) subject to the constraints that NOMA has a lower MSE than OMA.

The Karush Kuhn Tucker (KKT) result [2] is shown in (9) at the bottom of this page.

$$
\begin{aligned}
&D_{\alpha} f\left(\alpha_{m,1}^{DL}\right) \\
&= -b_1^{DL} \frac{\frac{1}{\ln 2} \frac{\eta P_{max}\left|H_{m,1}^{DL}\right|^2}{P_{N_0}^{DL}+\eta P_{max}\alpha_{m,1}^{DL}\left|H_{m,1}^{DL}\right|^2}}{\left(\log_2\left(1+\frac{\eta P_{max}\alpha_{m,1}^{DL}\left|H_{m,1}^{DL}\right|^2}{P_{N_0}^{DL}}\right)+c_1^{DL}\right)^2} \\
&\quad -b_2^{DL} \frac{\frac{1}{\ln 2} \frac{\eta\left|H_{m,2}^{DL}\right|^2 P_{max}}{\left|H_{m,2}^{DL}\right|^2\alpha_{m,1}^{DL}P_{max}+\eta\left|H_{m,2}^{DL}\right|^2\left(1-\alpha_{m,1}^{DL}\right)P_{max}}}{\left(\log_2\left(1+\frac{\eta\left|H_{m,2}^{DL}\right|^2\left(1-\alpha_{m,1}^{DL}\right)P_{max}}{\left|H_{m,2}^{DL}\right|^2\alpha_{m,1}^{DL}P_{max}+P_{N_0}^{DL}}\right)+c_2^{DL}\right)^2} = 0,
\end{aligned}
\tag{9}
$$

$A_k^{(i),DL}$ denotes the set of subcarriers assigned to user k at the i-th iteration. It is assumed that $r_k^{*,DL}$ denotes the sum of all subcarriers information rates after power allocation. From the subcarriers allocated by user k, the aggregated information rate is:

$$
r_k^{*,DL} = \sum\nolimits_{A_k^{(i),DL}} R_{m,k}^{DL}, \tag{10}
$$

We can obtain the slope by computing the k-th user:

$$
S_k^{DL} = \left.\frac{d\frac{b_k^{DL}}{r_k^{DL}+c_k^{DL}}}{dr_k^{DL}}\right|_{r_k^{DL}=r_{k^*,DL}} = -\frac{b_k^{DL}}{\left(r_k^{*,DL}+c_k^{DL}\right)^2}, \tag{11}
$$

If the user's slope is steeper, this means that the MSE decreases more when one additional subcarrier is obtained. We then select the user $k^{*,DL}$ with the minimal (steepest) slope, which is $k^{*,DL} = \arg\min\left\{S_k^{DL}\right\}$ to obtain the subcarrier.

3) Iterative Subcarrier Reassignment: After power allocation and calculation of the RD function slope, we consider the video MSE to reassign the subcarrier in the application layer. We try to reassign each subcarrier m to user $k^{*,DL}$.

It is assumed that Ω^{DL} is the set of users with the potential to improve the video quality by receiving extra subcarriers. We initialize the set $\Omega^{DL} = \{1, 2, 3 \ldots K\}$. It is also assumed that $\rho_{m,1}^{(i),DL}$ (strong user) and $\rho_{m,2}^{(i),DL}$ (weak user) are the users assigned to subcarrier m at the i-th iteration.

We define $-\Delta^{DL}_{\rho_{m,n}^{(i),DL},m,n}$ as the MSE performance change for the user $\rho_{m,n}^{(i),DL}$ losing the subcarrier. $k^{*(i),DL}$ is the user with the steepest slope in the i-th iteration. We define $\Delta^{DL}_{k_n^{*(i),DL},m}$ as the MSE performance gain of the subcarrier for the user $k^{*(i),UL}$ which replaces the user $\rho_{m,n}^{(i),DL}$. It is calculated that $-\Delta^{DL}_{\rho_{m,n(i),DL},m,n} < 0$, and $\Delta^{DL}_{k_n^{*(i),DL},m} > 0$.

If $(\Delta^{DL}_{k_n^{*(i),DL},m^*} - \Delta^{DL}_{\rho_{m,n}^{(i),DL},m,n^*}) > 0, \forall n = \{1, 2, 3 \ldots N\}$, we will find the largest one and reassign the largest pairing's subcarrier m^* to user $k^{*(i),DL}$ in the $i+1$ th iteration, i.e. $\rho_{m,n}^{(i+1),DL} = k^{*(i),DL}$. We then recalculate the slope with the new allocation and return to Step (3) with the new slope to update the user $k^{*(i+1),DL}$ with the lowest slope.

If all the $(\Delta^{DL}_{k_n^{*(i),DL},m^*} - \Delta^{DL}_{\rho_{m,n}^{(i),DL},m,n^*}) < 0, n = \{1, 2, 3 \ldots N\}$, we find that reassigning any subcarrier to the user $k^{*,DL}$ will not improve the overall performance. We then return to Step (2) to update user $k^{*(i+1),DL}$ with the second steepest slope. At the same time, the user $k^{*(i),DL}$ used in the i-th iteration will not be included in the $i+1$th iteration of the exchange, i.e. we remove $k^{*(i),DL}$ from Ω^{DL} until no user $k^{*,DL}$ can be allocated (i.e. the Ω^{DL} set becomes empty).

A. COMPUTATIONAL COMPLEXITY OF THE SUBCARRIER ALLOCATION AND USER GROUPING

The above subcarrier allocation and user grouping algorithm has the following computational complexity. In step (1), the sorting of the channel responses of K users on each of M subcarrier has the complexity $O(M^*K\log_2 K)$. The user k with the steepest slope tries to replace two users of all M subcarriers, so the complexity is O(2M). Denote the number of iterations among step (2) and step (3) is L. L is many times of K because one user with steepest RD slope tries to rob a subcarrier from the other users at each iteration and often one user can gain subcarrier many times. Finally, the sum computational complexity of the subcarrier allocation and user grouping algorithm is $O(M^*K\log_2 K+2M^*L)$. Due to the high complexity of the iterative nature of the previous scheme [2] (large L), we are motivated to propose deep neural network-based subcarrier assignment/user grouping in the next section which is non-iterative and the iterative part of the computational complexity can be saved.

V. PROPOSED DEEP NEURAL NETWORK-BASED SUBCARRIER ASSIGNMENT/USER GROUPING

The subcarrier assignment/NOMA user grouping results in the previous section are used as training (labeled) data in this section.

A. TRAINING PROCESS

The channel gains $H_{m,k}^{DL}$ are normalized to give zero mean and unit variance, as in [50]. The normalized channel gains $\hat{H}_{m,k}^{DL}$ can be written as:

$$\hat{H}_{m,k}^{DL} = \frac{log_{10}H_{m,k}^{DL} - E[log_{10}H_{m,k}^{DL}]}{\sqrt{E[(log_{10}H_{m,k}^{DL} - E[log_{10}H_{m,k}^{DL}])^2]}} \quad (12)$$

We employ the normalized channel gain as the input to the DNN. The input data can be denoted as $\mathrm{X} = \left[\hat{H}_{1,1}^{DL}, \ldots, \hat{H}_{M,K}^{DL}\right]$, and the output of the DNN is the assignment of the users to the subcarriers, which can be denoted as $Y = [u_{1,1}, u_{1,2}, \ldots, u_{1,K}, u_{2,1}, u_{2,2}, \ldots, u_{2,K}, \ldots, u_{M,K}]$, where each element is 0 or 1 s.

We use θ to denote the set of all the parameters of the network, $\theta = \{\theta_1, \theta_2, \ldots, \theta_{\mathrm{L}}\}$. The set of the parameters of the l-th layer is denoted $\theta_l = \{\mathrm{W}_l, \mathrm{b}_l\}$.The l-th layer can be written as:

$$Y_l = \sigma(W_l X_l + b_l) \quad (13)$$

where $\sigma(\cdot)$ is an activation function. At each layer except the last, we use the rectified linear unit (ReLU) function with $\sigma(\mathrm{x}) = \max(0, \mathrm{x})$ as the activation function, as this keeps the gradient at one; in this way, the size of the gradients is not exponentially reduced as we backpropagate through many layers. ReLU usually learns more quickly in DNN, allowing training of a deep supervised network without unsupervised pre-training [60].

In the last layer, a sigmoid function $\sigma(x) = \frac{1}{1+e^{-x}}$ is used to map the output to the interval [0,1]. The input and output mapping of the L-layer DNN is the series of functions expressed in (14) at the bottom of the previous page.

$$Y_L = \sigma\left(W_L \ldots K(\sigma\left(W_2\sigma\left(W_1 + X_1 + b_1\right)\right) + b_2) \ldots K + b_L\right) \quad (14)$$

$$Loss\,(W, b) = \frac{1}{MK}\sum_{i}^{MK} -[Y\,(i)\ln\left(Y_L\,(i)\right) + (1 - Y\,(i))\ln\left(1 - Y_L(i)\right)] \quad (15)$$

We use binary cross entropy (BCE) between the DNN output Y_L and desired output Y^* as the cost function expressed in (9) at the bottom of the previous page..

B. ADAM OPTIMIZER

We use a first-order gradient-based optimization algorithm for stochastic objective functions, such as the Adam optimizer, to gradually adjust the W and b according to the cost function. To adjust W (b is adjusted similarly),

$$u_t = \beta_1 u_{t-1} + (1 - \beta_1)\frac{\partial Loss_t}{\partial W_t} \quad (16)$$

$$v_t = \beta_1 v_{t-1} + (1 - \beta_2)\left(\frac{\partial Loss_t}{\partial W_t}\right)^2 \quad (17)$$

	1	2	3	4
1	0.401091	0.243539	0.608388	0.245658
2	0.216548	0.075957	0.347505	0.743452
3	0.399518	0.21241	0.857284	0.448317
4	0.98139	0.776981	0.575736	0.880566

FIGURE 3. DNN output before the conversion algorithm (rows represent users, and columns subcarriers).

$$\hat{u}_t = \frac{u_t}{1 - \beta_1^t} \quad (18)$$

$$\hat{v}_t = \frac{v_t}{1 - \beta_2^t} \quad (19)$$

$$W_{t+1} = W_t - \gamma\frac{\hat{u}_t}{\sqrt{\hat{v}_t} + \epsilon}. \quad (20)$$

We update the biased first moment estimate u_t and biased second moment estimate v_t. β_1 is the exponential decay rate for the first moment and β_2 is the exponential decay rate for the second moment. u_t is then initialized to zero. The bias correction of the gradient mean u_t is denoted as $\hat{u}_t$, and similarly for $\hat{v}_t$. γ is the learning rate, and ϵ is a small value to avoid the denominator being zero, often 10^{-8}.

C. DROPOUT

Dropout is a technique for reducing the overfitting problem in neural networks. The primary purpose is to randomly drop units from the neural networks in either the hidden or visible layers during training. This can prevent the over-fitting problem.

D. DNN OUTPUT LAYER CONVERSION ALGORITHM TO MEET CONSTRAINTS

During the testing stage (following the training stage), we need to convert the sigmoid probability (a value between [0,1]) learned by DNN into zero or one (i.e. unassigned or assigned). The subcarrier allocation/NOMA user grouping needs to meet two constraints: (i) there must be at least one subcarrier for each user; and (ii) there must be two users on each subcarrier. We therefore propose the following conversion algorithm, and use Figs. 3–6 to give an example of the post-processing, showing how the actual subcarrier assignment takes place.

Step 1. We sort the DNN output in Fig. 3 (values between [0,1] due to the sigmoid activation function) in descending order, as shown in Fig. 4. There are circles around the rank numbers. For example, ① (rank 1) is (4,1), indicating the element in row 4 and column 1 of Fig. 3, i.e. 0.98139.

Step 2. According to Constraint 1, each user has one subcarrier. The subcarrier allocation matrix Fig. 5 whose all components are all zeros initially shows the process and the result of step 2. In Fig. 5, 1 at (i,j) component indicates subcarrier j is assigned to user i and the number with a circle around it indicate the rank number (also step number).

	user	subcarrier
①	4	1
②	4	4
③	3	3
④	4	2
⑤	2	4
⑥	1	3
⑦	4	3
⑧	3	4
⑨	1	1
⑩	3	1
⑪	2	3
⑫	1	4
⑬	1	2
⑭	2	1
⑮	3	2
⑯	2	2

FIGURE 4. Sorting of Fig. 3 in descending order. The rank is shown as a number within a circle. For example, The DNN output of User 4 and Subcarrier 1 is ① (ranked first).

	1	2	3	4
1	0	0	1⑥	0
2	0	0	0	1⑤
3	0	0	1③	0
4	1①	0④	0	0②

FIGURE 5. The subcarrier allocation matrix (rows represent users, and columns represent subcarriers) after step 2. Each user has one subcarrier to satisfy constraint 1.

We start with ① (user 4 subcarrier 1 in Fig. 4), let user 4 have subcarrier 1, and thus the (4,1) component of Fig. 5 becomes 1. We then move to (user 4 subcarrier 4 in Fig. 4), but user 4 already has subcarrier 1, so we skip ②, and thus we mark (4,4) component of Fig. 5 with a cross. The process continues until all users have one subcarrier. Note that ④-(4,2) component is crossed out (skipped) since this user already has one subcarrier.

Step 3. To satisfy Constraint 2, we also choose from ① to ⑯ of Fig. 4, but skip those already chosen in Step 2 (①, ③, ⑤, and ⑥). If this does not meet Constraint 2, we skip to the next one. The process continues until each subcarrier has two users (i.e. Constraint 2 is satisfied). Fig. 6 shows the process and the result of step 3. We see that ⑦, ⑧, ⑩, ⑪, and are crossed out (skipped) since Constraint 2 is violated. Specifically, the ⑦- (4,3) component is crossed out because subcarrier 3 already has two users: user 3 (③) and user 1 (⑥).

	1	2	3	4
1	1⑨	1⑬	1⑥	0⑫
2	0	0	0⑪	1⑤
3	0⑩	0	1③	0⑧
4	1①	1④	0⑦	1②

FIGURE 6. The subcarrier allocation matrix (rows represent users, and columns represent subcarriers) after step 3. Each subcarrier has two users to satisfy Constraint 2.

TABLE 2. DNN parameters.

Parameter	Value
K (users)	4
M (subcarrier)	4
BW (bandwidth of each subcarrier)	200kHz
Learning rate	0.0001
Dropout rate	0.5
Activation function	ReLU
Activation function at the last layer	Sigmoid
Cost function	binary cross entropy
Training data	20000
Epochs	2000
Hidden layers	3
Number of neurons	256/512/256

VI. SIMULATION RESULTS

The parameters for the DNN are listed in Table 2. The number of epochs is equal to 2,000, since the model converges within 2,000 epochs. We compare the following schemes:

Scheme A [22] OFDMA (OMA) cross-layer resource allocation.

Scheme B [13] OFDMA/NOMA physical layer only resource allocation. Suboptimal user grouping (physical layer only), optimal power allocation (sum rate).

Scheme C ([2], described in Sec. IV in this paper): our previous work, non-DNN-based, iterative cross-layer subcarrier assignment/user grouping for OFDMA/NOMA video communication systems, optimal power allocation (sum video distortion).

Scheme D (Sec. V in this paper): the proposed DNN-based subcarrier assignment/user grouping plus optimal power allocation (sum video distortion) from [2] for OFDMA/NOMA video communication systems. The DNN uses Scheme C's subcarrier assignment/ user grouping results as training data.

For Scheme D, the volume of the used training data is 20000 since larger data volume does not improve the performance. The training data do not have the data

TABLE 3. Average PSNR (video quality) of schemes A-D, four users, four subcarriers, SNR = 15 DB.

	A	B	C	D
Mean	39.87772	37.08282	40.37562	40.17346
Standard deviation	0.156522	0.113649	0.063644	0.046751

imbalance problem in [61] because we randomly generated the channel coefficients of users at subcarriers as the DNN input, and apply Scheme C's subcarrier assignment/ user grouping results as the DNN desired output.

The video quality PSNR comparison, including mean and standard deviation) is shown in Table 3. Scheme A is better than Scheme B, since it considers both the application layer and the physical layer. Scheme C is better than Scheme A due to the use of NOMA. The performance loss of the proposed DNN-based Scheme D with respect to Scheme C is only 0.2 dB in PSNR. The complexity is lower due to the non-iterative approach used in Scheme D. For comparison, Scheme C has iterative steps – 3) iterative subcarrier reassignment in Sec. IV. In all schemes, the standard deviation is not significant.

ACKNOWLEDGMENT

The authors thank Mr. Cheng-Yu Yu for helpful discussions about DNN output layer conversion algorithm to meet two constraints.

VII. CONCLUSION

This paper has applied a DNN and supervised learning to a subcarrier assignment and user grouping problem in an OFDMA/NOMA downlink video transmission system. By replacing the original iterative method, we have shown that the proposed deep learning technique can achieve a similar (although slightly poorer) result, with low complexity.

ABBREVIATIONS

3GPP	Third-generation partnership project
4G	Fourth-generation mobile system
5G	Fifth-generation mobile system
ADC	Analogue-to-digital conversion
ATSC	Advanced television systems committee
BCE	Binary cross entropy
BS	Base station
BW	Bandwidth of each subcarrier
CNN	Convolutional neural network
CoMP	Coordinated multipoint
CP	Cyclic prefix
CSI	Channel state information
DAC	Digital-to-analogue conversion
DL	Downlink
D2D	Device-to-device
DNN	Deep neural network
FFT	Fast Fourier transform
GOP	Group of pictures
IFFT	Inverse fast Fourier transform
IP	Internet protocol
LSTM	Long short-term memory
LTE-U	Long term evolution-unlicensed
ML	Machine learning
MSE	Mean square error
NOMA	Non-orthogonal multiple access
NP	Non-deterministic polynomial time
OFDMA	Orthogonal frequency division multiple access
OMA	Orthogonal multiple access
PSNR	Peak signal-to-noise ratio
QoS	Quality of service
RBM	Restricted Boltzmann machine
RD	Rate distortion
ReLU	Rectified linear unit
RNN	Recurrent neural network
SE	Spectrum efficiency
SER_t	Target symbol error rate
SIC	Successive interference cancellation
SINR	Signal-to-noise plus interference ratio
UL	Uplink
WMMSE	Weighted minimum mean square error

REFERENCES

[1] G. Gui, H. Huang, Y. Song, and H. Sari, "Deep learning for an effective nonorthogonal multiple access scheme," *IEEE Trans. Veh. Technol.*, vol. 67, no. 9, pp. 8440–8450, Sep. 2018.

[2] S.-M. Tseng, W.-D. Tsai, and H.-S. Suo, "Cross-layer 1 and 5 user grouping/power allocation/subcarrier allocations for downlink OFDMA/NOMA video communications," *Int. J. Commun. Syst.*, vol. 32, no. 14, p. e4084, Sep. 2019.

[3] Z. Ding, Y. Liu, J. Choi, Q. Sun, M. Elkashlan, C.-L. I, and H. V. Poor, "Application of non-orthogonal multiple access in LTE and 5G networks," *IEEE Commun. Mag.*, vol. 55, no. 2, pp. 185–191, Feb. 2017.

[4] L. Zhang, W. Li, Y. Wu, X. Wang, S.-I. Park, H. M. Kim, J.-Y. Lee, P. Angueira, and J. Montalban, "Layered-division-multiplexing: Theory and practice," *IEEE Trans. Broadcast.*, vol. 62, no. 1, pp. 216–232, Mar. 2016.

[5] S. M. R. Islam, N. Avazov, O. A. Dobre, and K.-S. Kwak, "Power-domain non-orthogonal multiple access (NOMA) in 5G systems: Potentials and challenges," *IEEE Commun. Surveys Tuts.*, vol. 19, no. 2, pp. 721–742, 2nd Quart., 2017.

[6] "3GPP release 15 overview," *IEEE Spectr.* [Online]. Available: https://spectrum.ieee.org/telecom/wireless/3gpp-release-15-overview

[7] Y. Liu, Z. Qin, M. Elkashlan, Z. Ding, A. Nallanathan, and L. Hanzo, "Nonorthogonal multiple access for 5G and beyond," *Proc. IEEE*, vol. 105, no. 12, pp. 2347–2381, Dec. 2017.

[8] M. Bennis, M. Debbah, and H. V. Poor, "Ultrareliable and low-latency wireless communication: Tail, risk, and scale," *Proc. IEEE*, vol. 106, no. 10, pp. 1834–1853, Oct. 2018.

[9] *Cisco Visual Networking Index: Forecast and Trends, 2017–2022*. Accessed: Nov. 26, 2018. [Online]. Available: https://www.cisco.com/c/en/us/solutions/collateral/service-provider/visual-networking-index-vni/white-paper-c11-741490.html#_Toc529314172

[10] L. Lei, D. Yuan, C. K. Ho, and S. Sun, "Power and channel allocation for non-orthogonal multiple access in 5G systems: Tractability and computation," *IEEE Trans. Wireless Commun.*, vol. 15, no. 12, pp. 8580–8594, Dec. 2016.

[11] R. Singh, "Sub-channel assignment and resource scheduling for non-orthogonal multiple access (NOMA) in downlink coordinated multi-point systems," in *Proc. 20th Conf. Innov. Clouds, Internet Netw. (ICIN)*, Paris, France, Mar. 2017, pp. 17–22.

[12] M. Al-Imari, P. Xiao, M. A. Imran, and R. Tafazolli, "Uplink non-orthogonal multiple access for 5G wireless networks," in *Proc. 11th Int. Symp. Wireless Commun. Syst. (ISWCS)*, Barcelona, Spain, Aug. 2014, pp. 781–785.

[13] M. S. Ali, H. Tabassum, and E. Hossain, "Dynamic user clustering and power allocation for uplink and downlink non-orthogonal multiple access (NOMA) systems," *IEEE Access*, vol. 4, pp. 6325–6343, 2016.

[14] H.-S. Lang, S.-C. Lin, and W.-H. Fang, "Subcarrier pairing and power allocation with interference management in cognitive relay networks based on genetic algorithms," *IEEE Trans. Veh. Technol.*, vol. 65, no. 9, pp. 7051–7063, Sep. 2016.

[15] W.-C. Pao, Y.-F. Chen, and M.-G. Tsai, "An adaptive allocation scheme in multiuser OFDM systems with time-varying channels," *IEEE Trans. Wireless Commun.*, vol. 13, no. 2, pp. 669–679, Feb. 2014.

[16] W.-C. Pao, W.-B. Wang, S.-M. Tseng, and Y.-F. Chen, "A resource allocation scheme with fractional frequency reuse in multi-cell OFDMA systems," *Wireless Pers. Commun.*, vol. 101, no. 4, pp. 2009–2027, Aug. 2018.

[17] S.-L. Wu and W.-W. Wang, "Energy-efficient multimedia multicast scheduling and resource allocation algorithms for OFDMA-based systems," in *Proc. CIT/IUCC/DASC/PICom*, Liverpool, U.K., Oct. 2015, pp. 1377–1382.

[18] D. Liu, H. Cui, J. Wu, and C. Luo, "Resource allocation for uncoded multi-user video transmission over wireless networks," *Mobile Netw. Appl.*, vol. 21, no. 6, pp. 950–961, Dec. 2016.

[19] G.-M. Su, Z. Han, M. Wu, and K. J. R. Liu, "A scalable multiuser framework for video over OFDM networks: Fairness and efficiency," *IEEE Trans. Circuits Syst. Video Technol.*, vol. 16, no. 10, pp. 1217–1231, Oct. 2006.

[20] S. Cicalo and V. Tralli, "Distortion-fair cross-layer resource allocation for scalable video transmission in OFDMA wireless networks," *IEEE Trans. Multimedia*, vol. 16, no. 3, pp. 848–863, Apr. 2014.

[21] K. Lin and S. Dumitrescu, "Cross-layer resource allocation for scalable video over OFDMA wireless networks: Tradeoff between quality fairness and efficiency," *IEEE Trans. Multimedia*, vol. 19, no. 7, pp. 1654–1669, Jul. 2017.

[22] D. Wang, L. Toni, P. C. Cosman, and L. B. Milstein, "Uplink resource management for multiuser OFDM video transmission systems: Analysis and algorithm design," *IEEE Trans. Commun.*, vol. 61, no. 5, pp. 2060–2073, May 2013.

[23] Y.-F. Chen, S.-M. Tseng, C.-H. Shen, and M.-S. He, "Cross layer 1, 2 and 5 resource allocation in uplink turbo-coded HARQ based OFDMA video transmission systems," *Wireless Pers. Commun.*, vol. 98, no. 2, pp. 1997–2008, Feb. 2018.

[24] S.-M. Tseng, Y.-F. Chen, P.-H. Chiu, and H.-C. Chi, "Jamming resilient cross-layer resource allocation in uplink HARQ-based SIMO OFDMA video transmission systems," *IEEE Access*, vol. 5, pp. 24908–24919, Dec. 2017.

[25] S.-M. Tseng and Y.-F. Chen, "Average PSNR optimized cross layer user grouping and resource allocation for uplink MU-MIMO OFDMA video communications," *IEEE Access*, vol. 6, pp. 50559–50571, Dec. 2018.

[26] G. E. Hinton, L. Deng, D. Yu, G. Dahl, A. Mohamed, N. Jaitly, and T. Sainath, "Deep neural networks for acoustic modeling in speech recognition," *IEEE Signal Process. Mag.*, vol. 29, no. 6, pp. 82–97, Oct. 2012.

[27] A. Krizhevsky, L. Sutskever, and G. E. Hinton, "ImageNet classification with deep convolutional neural networks," in *Proc. Adv. Neural Inf. Process. Syst.*, Lake Tahoe, NV, USA, 2012, pp. 1090–1098.

[28] Y. LeCun, Y. Bengio, and G. Hinton, "Deep learning," *Nature*, vol. 521, pp. 436–444, May 2015.

[29] G. E. Hinton, S. Osindero, and Y.-W. Teh, "A fast learning algorithm for deep belief nets," *Neural Comput.*, vol. 18, no. 7, pp. 1527–1554, 2006.

[30] J. Shin, "Deep learning for optimization, communication and networks," in *Proc. East Asian School Inf. Theory Commun. (EASITC)*, Taipei, Taiwan, Aug. 2018.

[31] Y. LeCun, B. E. Boser, J. S. Denker, D. Henderson, R. E. Howard, W. E. Hubbard, and L. D. Jackel, "Handwritten digit recognition with a back-propagation network," in *Proc. Adv. Neural Inf. Process. Syst.*, 1990, pp. 396–404.

[32] Y. LeCun, L. Bottou, Y. Bengio, and P. Haffner, "Gradient-based learning applied to document recognition," *Proc. IEEE*, vol. 86, no. 11, pp. 2278–2324, Nov. 1998.

[33] P. J. Werbos, "Backpropagation through time: What it does and how to do it," *Proc. IEEE*, vol. 78, no. 10, pp. 1550–1560, Oct. 1990.

[34] K. Cho, B. Van Merriënboer, and C. Gulcehre, "Learning phrase representations using RNN encoder-decoder for statistical machine translation," in *Proc. Conf. Empirical Methods Natural Lang. Process.*, Doha, Qatar, 2014, pp. 1724–1734.

[35] S. Hochreiter and J. Schmidhuber, "Long short-term memory," *Neural Comput.*, vol. 9, no. 8, pp. 1735–1780, Nov. 1997.

[36] T. Gruber, S. Cammerer, J. Hoydis, and S. ten Brink, "On deep learning-based channel decoding," in *Proc. 51st Annu. Conf. Inf. Sci. Syst. (CISS)*, Baltimore, MD, USA, Mar. 2017, pp. 1–6.

[37] T. O'Shea and J. Hoydis, "An introduction to deep learning for the physical layer," *IEEE Trans. Cogn. Commun. Netw.*, vol. 3, no. 4, pp. 563–575, Oct. 2017.

[38] M. Kim, N.-I. Kim, W. Lee, and D.-H. Cho, "Deep learning-aided SCMA," *IEEE Commun. Lett.*, vol. 22, no. 4, pp. 720–723, Apr. 2018.

[39] H. Ye, G. Y. Li, and B.-H. Juang, "Power of deep learning for channel estimation and signal detection in OFDM systems," *IEEE Wireless Commun. Lett.*, vol. 7, no. 1, pp. 114–117, Feb. 2018.

[40] Q. Mao, F. Hu, and Q. Hao, "Deep learning for intelligent wireless networks: A comprehensive survey," *IEEE Commun. Surveys Tuts.*, vol. 20, no. 4, pp. 2595–2621, 4th Quart., 2018.

[41] K. I. Ahmed, H. Tabassum, and E. Hossain, "Deep learning for radio resource allocation in multi-cell networks," Aug. 2018, *arXiv:1808.00667*. [Online]. Available: https://arxiv.org/abs/1808.00667

[42] Y. Sun, M. Peng, Y. Zhou, and Y. Huang, "Application of machine learning in wireless networks: Key techniques and open issues," Sep. 2018, *arXiv:1809.08707*. [Online]. Available: https://arxiv.org/abs/1809.08707

[43] V. Singhal, J. Maggu, and A. Majumdar, "Simultaneous detection of multiple appliances from smart-meter measurements via multi-label consistent deep dictionary learning and deep transform learning," *IEEE Trans. Smart Grid*, vol. 10, no. 3, pp. 2969–2978, May 2019.

[44] S. Chakrabarty and E. A. P. Habets, "Multi-speaker DOA estimation using deep convolutional networks trained with noise signals," *IEEE J. Sel. Topics Signal Process.*, vol. 13, no. 1, pp. 8–21, Mar. 2019.

[45] S. Yu, X. Wang, and R. Langar, "Computation offloading for mobile edge computing: A deep learning approach," in *Proc. IEEE 28th Annu. Int. Symp. Pers., Indoor, Mobile Radio Commun. (PIMRC)*, Montreal, QC, Canada, Oct. 2017, pp. 1–6.

[46] H. Sun, X. Chen, Q. Shi, M. Hong, X. Fu, and N. D. Sidiropoulos, "Learning to optimize: Training deep neural networks for wireless resource management," in *Proc. IEEE 18th Int. Workshop Signal Process. Adv. Wireless Commun. (SPAWC)*, Sapporo, Japan, Jul. 2017, pp. 1–6.

[47] Z. Xu, Y. Wang, J. Tang, J. Wang, and M. C. Gursoy, "A deep reinforcement learning based framework for power-efficient resource allocation in cloud RANs," in *Proc. IEEE Int. Conf. Commun. (ICC)*, Paris, France, May 2017, pp. 1–6.

[48] U. Challita, L. Dong, and W. Saad, "Proactive resource management for LTE in unlicensed spectrum: A deep learning perspective," *IEEE Trans. Wireless Commun.*, vol. 17, no. 7, pp. 1674–1689, Jul. 2018.

[49] M. I. Khan, M. M. Alam, Y. Le Moullec, and E. Yaacoub, "Cooperative reinforcement learning for adaptive power allocation in device-to-device communication," in *Proc. IEEE 4th World Forum Internet Things (WF-IoT)*, Singapore, Feb. 2018, pp. 476–481.

[50] W. Lee, "Resource allocation for multi-channel underlay cognitive radio network based on deep neural network," *IEEE Commun. Lett.*, vol. 22, no. 9, pp. 1942–1945, Sep. 2018.

[51] W. Lee, M. Kim, and D.-H. Cho, "Deep power control: Transmit power control scheme based on convolutional neural network," *IEEE Commun. Lett.*, vol. 22, no. 6, pp. 1276–1279, Jun. 2018.

[52] X. Li, J. Fang, W. Cheng, H. Duan, Z. Chen, and H. Li, "Intelligent power control for spectrum sharing in cognitive radios: A deep reinforcement learning approach," *IEEE Access*, vol. 6, pp. 25463–25473, Apr. 2018.

[53] A. Zappone, M. Debbah, and Z. Altman, "Online energy-efficient power control in wireless networks by deep neural networks," in *Proc. IEEE Workshop Signal Process. Adv. Wireless Commun. (SPAWC)*, Kalamata, Greece, Jun. 2018, pp. 1–5.

[54] J. Luo, J. Tang, D. K. C. So, G. Chen, K. Cumanan, and J. A. Chambers, "A deep learning-based approach to power minimization in multi-carrier NOMA with SWIPT," *IEEE Trans. Signal Process.*, vol. 7, pp. 17450–17460, 2019.

[55] Y. Sun, Y. Wang, J. Jiao, S. Wu, and Q. Zhang, "Deep learning-based long-term power allocation scheme for NOMA downlink system in S-IoT," *IEEE Access*, vol. 7, pp. 86288–86296, Jul. 2019.

[56] S. Wang, H. Liu, P. H. Gomes, and B. Krishnamachari, "Deep reinforcement learning for dynamic multichannel access in wireless networks," *IEEE Trans. Cogn. Commun. Netw.*, vol. 4, no. 2, pp. 257–265, Jun. 2018.

[57] M. Liu, T. Song, J. Hu, J. Yang, and G. Gui, "Deep learning-inspired message passing algorithm for efficient resource allocation in cognitive radio networks," *IEEE Trans. Veh. Technol.*, vol. 68, no. 1, pp. 641–653, Jan. 2019.

[58] Z.-M. Chen, X.-S. Wei, P. Wang, and Y. Guo, "Multi-label image recognition with graph convolutional networks," in *Proc. IEEE Conf. Comput. Vis. Pattern Recognit.*, Jun. 2019, pp. 5177–5186.
[59] K. Stuhlmuller, N. Farber, M. Link, and B. Girod, "Analysis of video transmission over lossy channels," *IEEE J. Sel. Areas Commun.*, vol. 18, no. 6, pp. 1012–1032, Jun. 2000.
[60] X. Glorot, A. Bordes, and Y. Bengio, "Deep sparse rectifier neural networks," in *Proc. 14th Int. Conf. Artif. Intell. Statist.*, Fort Lauderdale, FL, USA, 2011, pp. 315–323.
[61] X.-Y. Jing, X. Zhang, X. Zhu, F. Wu, X. You, Y. Gao, S. Shan, and J.-Y. Yang, "Multiset feature learning for highly imbalanced data classification," *IEEE Trans. Pattern Anal. Mach. Intell.*, to be published, doi: 10.1109/TPAMI.2019.2929166.

SHU-MING TSENG received the B.S. degree in electrical engineering from National Tsing Hua University, Taiwan, in 1994, and the M.S. and Ph.D. degrees in electrical engineering from Purdue University, IN, USA, in 1995 and 1999, respectively. From 1999 to 2001, he was with the Department of Electrical Engineering, Chang Gung University, Taiwan. Since 2001, he has been with the Department of Electronic Engineering, National Taipei University of Technology, Taipei, Taiwan, where he has been a Professor, since 2007. He is also the author of 48 SCI journal articles, including 14 in IEEE. His research interests include NOMA, MU-MIMO, OFDMA, deep learning-based radio resource allocation, cross layer optimization for video transmission, network performance evaluation, software-defined radio, and optical systems. He has served as an Editor for the *KSII Transactions on Internet and Information Systems*, from 2013 to 2019.

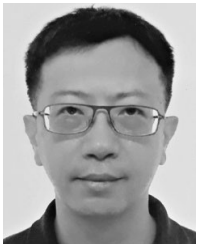

YUNG-FANG CHEN received the B.S. degree in computer science and information engineering from National Taiwan University, Taipei, Taiwan, in 1990, the M.S. degree in electrical engineering from the University of Maryland, College Park, in 1994, and the Ph.D. degree in electrical engineering from Purdue University, West Lafayette, IN, in 1998. From 1998 to 2000, he was with Lucent Technologies, Whippany, NJ, where he was with the CDMA Radio Technology Performance Group. Since 2000, he has been with the Faculty of the Department of Communication Engineering, National Central University, Taoyuan, Taiwan, where he is currently a Professor. His research interests include resource management algorithm designs for communication systems and signal processing algorithm designs for wireless communication systems.

CHENG-SHUN TSAI received the M.S. degree in electronic engineering from the Department of Electronic Engineering, National Taipei University of Technology, Taiwan, in 2019. His research interests include deep learning-based resource management for OFDMA/NOMA video communication systems.

WEN-DA TSAI received the M.S. degree in electronic engineering from the Department of Electronic Engineering, National Taipei University of Technology, Taiwan, in 2018. His research interests include cross-layer resource management for OFDMA/NOMA video communication systems. He is currently with the Division of Software 9, Compal Electronics, Inc., Taipei, Taiwan.